Spectral Analysis of 1.55-μm InAs–InP(113)B Quantum-Dot Lasers Based on a Multipopulation Rate Equations Model

Frédéric Grillot, *Member, IEEE*, Kiril Veselinov, *Member, IEEE*, Mariangela Gioannini, *Member, IEEE*, Ivo Montrosset, *Member, IEEE*, Jacky Even, Rozenn Piron, Estelle Homeyer, and Slimane Loualiche

***Abstract*—In this paper, a theoretical model is used to investigate the lasing spectrum properties of InAs–InP(113)B quantum dot (QD) lasers emitting at 1.55 μm. The numerical model is based on a multipopulation rate equations analysis. Calculations take into account the QD size dispersion as well as the temperature dependence through both the inhomogeneous and the homogeneous broadenings. This paper demonstrates that the model is capable of reproducing the spectral behavior of InAs–InP QD lasers. Especially, this study aims to highlight the transition of the lasing wavelength from the ground state (GS) to the excited state (ES). In order to understand how the QD laser turns on, calculated optical spectra are determined for different cavity lengths and compared to experimental ones. Unlike InAs–GaAs QD lasers emitting at 1.3 μm, it is shown that a continuous transition from the GS to the ES is exhibited because of the large inhomogeneous broadening comparable to the GS and ES lasing energy difference.**

***Index Terms*—Quantum dot (QD), rate equation, semiconductor laser.**

I. Introduction

LOW-COST, directly modulated lasers will play a major role in the next generation telecommunication links (local and metropolitan area network) for uncooled and isolator-free applications. As a consequence, semiconductor lasers based on low-dimensional heterostructures such as quantum dot (QD) laser are very promising. Indeed, QD structures have attracted a lot of attention in the last decade since they exhibit many interesting and useful properties such as low threshold current [1], temperature insensitivity [2], chirpless behavior [3], and optical feedback resistance [4]. Thus, thanks to QD lasers, several steps toward cost reduction can be reached as improving the laser resistance to temperature fluctuation in order to remove temperature control elements (Peltier cooler), or designing feedback resistant laser for isolator-free transmissions and optics-free module. Most investigations reported in the literature deal with InGaAs QD grown on GaAs substrates [5], [6]. However, it is important to stress that InGaAs—GaAs QD devices do not usually lead to a laser emission above 1.45 μm [7], which is detrimental for long-haul optical transmission. In order to reach the standards of long-haul transmissions, 1.55 μm InAs QD lasers grown on InP substrate have been developed. More particularly, it has been demonstrated that the use of the specific InP(113)B substrate orientation when combined with optimized growth techniques leads to very small (4 nm high) and dense (up to 10^{11} cm^{-2}) QD structures [8]. Recent experimental studies conducted on these devices have shown that a second laser peak occurs in the laser spectrum when increasing the injection power. This double laser emission is a common property found independently by different research groups both for InGaAs—GaAs and InAs—InP systems [9], [10]. The experimental results in [11] have even shown a saturation and complete rollover of the first emission after the occurrence of the excited state (ES) threshold, while an increasing behavior for both lasing wavelengths has been observed for an InAs—InP(113)B QD laser [9]. The origin of the double emission has been explained by the finite ground state (GS) relaxation time using a cascade relaxation model that brings the GS emission to a constant value after the ES threshold [12]. This approach has been also used to extract the dynamical properties of a QD laser [13], while the complete rollover has been attributed to an asymmetry in the thermal population redistribution [14]. A comparison between numerical results and experimental ones has recently been conducted by using either a cascade or a direct relaxation channel model [15]. Such a study has led to demonstrate that when a direct relaxation channel from the wetting layer (WL) to the GS is taken into account, the numerical results match very well the measurements and lead to a qualitative understanding of InAs–InP(113)B QD lasers. If no direct relaxation channel is assumed, a good agreement with the experimental results observed in the InAs/GaAs system is obtained.

The aim of this paper is now to investigate the lasing spectra behavior of 1.55 μm InAs–InP(113)B QD lasers. As a result, a model based on multipopulation rate equations is used. The paper is organized as follows: in Section II a description of the

Manuscript received September 14, 2008; revised November 20, 2008. Current version published May 28, 2009. This work was supported by ePIXnet (European Network of Excellence on Photonic Integrated Components and Circuits).

F. Grillot is with the Center for High Technology Materials (CHTM), University of New Mexico, Albuquerque, NM 87106 USA (e-mail: fgrillot@chtm.unm.edu). He is also with Fonctions Optiques pour les Technologies de l'informatiON-Institut National des Sciences Appliquées (FOTON-INSA), 35043 Rennes, France (e-mail: frederic.grillot@insa-rennes.fr).

K. Veselinov, J. Even, R. Piron, and S. Loualiche are with Fonctions Optiques pour les Technologies de l'informatiON-Institut National des Sciences Appliquées (FOTON-INSA), 35043 Rennes, France (e-mail: kiril.veselinov@ens.insa-rennes.fr; slimane.loualiche@insa-rennes.fr; jacky.even@insa-rennes.fr).

M. Gioannini and I. Montrosset are with Dipartimento di Elettronica, Politecnico di Torino, 10129 Torino, Italy (e-mail: mariangela.gioannini@polito.it; ivo.montrosset@polito.it).

E. Homeyer is with the Laboratory of Condensed Matter Physics and Nanostructures, Université Claude Bernard Lyon 1 and CNRS, 69622 Villeurbanne Cedex, France.

Digital Object Identifier 10.1109/JQE.2009.2013174

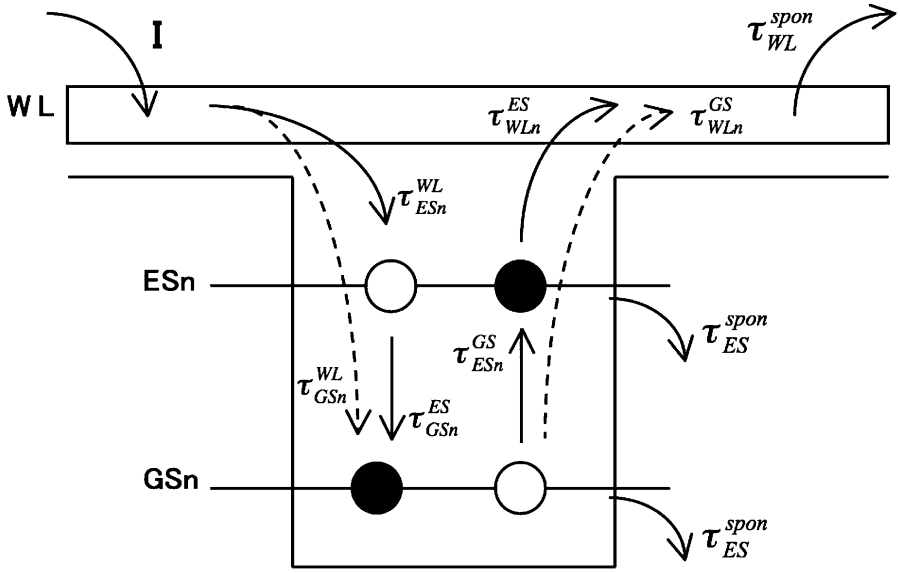

Fig. 1. Schematic representation of the carrier dynamics model with direct relaxation channel (dashed line) for the nth QD subgroup.

MPRE model is proposed. In order to take into account the inhomogeneous gain broadening of the QD ensemble, the various dot population, each characterized by a GS and an ES average energy level have to be considered as in [13]. Then, in Section III, numerical results are presented and compared to experimental ones. The modal gain is at first calculated both for the GS and the ES. When increasing pumping level, numerical results show that the device can emit on the GS only, on the two states or on the ES only. Optical spectra are then calculated considering a laser diode composed of an active region with two InAs QD layers. The transition from the GS to the ES influence is analyzed with respect to the laser cavity length. The calculated spectra are compared to experimental ones and found to be in good agreement each other. On the other hand, numerical results demonstrate that in the case of the InAs–InP system a continuous transition of the emitting wavelength from GS to ES is predicted. This situation is very different than the one observed in the InAs/GaAs system in which an abrupt transition is reported. Finally, we summarize our results and conclusions in Section IV.

This numerical model based on a multipopulation rate equation (MPRE) system is a powerful tool for the prediction of QD devices. Especially, taking into account a direct relaxation channel from the WL to the GS, this opens the way of predicting the behavior of InAs–InP(113)B QD lasers emitting at 1.55 μm. Good agreements with the experimental results, both for the case of the double laser emission as well as for the GS-lasing wavelength shift are demonstrated. This numerical investigation based on carrier dynamics is of prime importance for the optimization of low-cost sources for optical telecommunications as well as for a further improvement of QD laser performances at 1.55 μm on InP substrate, as already demonstrated for InAs–GaAs QDs at 1.3 μm [16], [17].

II. MPREs Model

In the following, a numerical model is used to study carrier dynamics in the two lowest energy levels of an InAs–InP(113)B QD system. Its active region consists of a QD ensemble with different dots interconnected with the WL. For simplicity, the existence of higher ESs is neglected and a common carrier reservoir is associated to both the WL and the barrier. In order to include the inhomogeneous broadening of the gain due the dot-size fluctuation the QD ensemble has been divided in n subgroups each characterized by an average energy of the ES E_{ESn}, and average energy of the GS E_{GSn}. The QD are assumed to be always neutral and electrons and holes are treated as eh-pairs and thermal effects and carrier losses in the barrier region are not taken into account. Fig. 1 shows a schematic representation of the carrier dynamics in the conduction band of the nth QD subgroup in the active region. First, an external carrier injection fills directly the WL reservoir with I being the injected current. Some of the eh-pairs are then captured on the fourfold degenerate ES of the QD ensemble with a capture time $\tau_{\mathrm{ESn}}^{\mathrm{WL}}$. Once on the ES, carriers can relax on the twofold GS ($\tau_{\mathrm{GSn}}^{\mathrm{ES}}$), be thermally reemitted in the WL reservoir ($\tau_{\mathrm{WLn}}^{\mathrm{ES}}$) or recombine spontaneously with a spontaneous emission time $\tau_{\mathrm{ES}}^{\mathrm{spon}}$ or by stimulated emission of photons with ES resonance energy. The same dynamic behavior is followed for the carrier population on the GS level with regard to the ES. This approach has been previously developed for the InAs–GaAs system [11] but in the case of InAs–InP(113)B system it is assumed that at low injection rates, the relaxation processes are phonon-assisted while the Auger effect dominates when the injection gets larger [18]. In order to include this effect, a modified model has been considered introducing a direct relaxation channel ($\tau_{\mathrm{GSn}}^{\mathrm{WL}}$) to the standard cascade relaxation model, as shown in Fig. 1 (dashed line). It is attributed to a single Auger process involving a WL electron captured directly into the GS by transferring its energy to a second WL electron [19]. Carriers are either captured from the WL reservoir into the ES or directly into the GS within the same time $\tau_{\mathrm{GSn}}^{\mathrm{WL}} = \tau_{\mathrm{ESn}}^{\mathrm{WL}}$.

This assumption has been made after analysis of the kinetic curves in [18] where the ES and GS population gave raise simultaneously 10 ps after excitation. On the other hand, carriers can also relax from the ES to the GS. The other transition mechanisms remain the same as in the cascade model. The capture and

the relaxation times are then calculated through a phenomenological relation depending on the carrier density in the WL reservoir [20], the ES and GS occupation probabilities, and the existence probability of the ES and GS transitions

$$\tau_{\mathrm{ESn}}^{\mathrm{WL}} = \frac{1}{(A_W + (C_W N_{\mathrm{WL}})/V_{\mathrm{WL}})\,(1 - P_{\mathrm{ESn}})G_{\mathrm{nES}}} \quad (1)$$

$$\tau_{\mathrm{GSn}}^{\mathrm{ES}} = \frac{1}{(A_E + (C_E N_{\mathrm{WL}})/V_{\mathrm{WL}})\,(1 - P_{\mathrm{GSn}})} \quad (2)$$

$$\tau_{\mathrm{GSn}}^{\mathrm{WL}} = \frac{1}{(A_W + (C_W N_{\mathrm{WL}})/V_{\mathrm{WL}})\,(1 - P_{\mathrm{GSn}})G_{\mathrm{nGS}}} \quad (3)$$

where N_{WL} is the carrier number in the WL reservoir, V_{WL} is the WL volume and $A_W(A_E), C_W(C_E)$ are the coefficients for phonon and Auger-assisted relaxation, respectively, related to the WL and the ES.

P_{ESn} and P_{GSn} are the filling probabilities of the ES and GS, respectively, in the nth subgroup of dots given by

$$P_{\mathrm{ESn,GSn}} = \frac{N_{\mathrm{ESn,GSn}}}{\mu_{\mathrm{ES,GS}} N_d w L_{\mathrm{ca}} N_l G_{\mathrm{nES,nGS}}} \quad (4)$$

with $N_{\mathrm{ESn,GSn}}$ being the ES and GS carrier number in the nth subgroup, $\mu_{\mathrm{ES,GS}}$ the degeneracy of the considered confined states, N_d the QD surface density, w and L_{ca} the width and length of the active region, and N_l being the number of QD layers. G_{nES} and G_{nGS} are the probabilities of recombination with E_{ESn} and E_{GSn} energy, respectively. To calculate them, a Gaussian QD size distribution has been considered with a consequent Gaussian distribution of the QD recombination energies. The eh-pairs escape times have been derived considering a Fermi distribution for the ES and GS carriers for the system in quasi-thermal equilibrium without external excitation [12]. To ensure this, the carrier escape time is related to the carrier capture time as follows:

$$\tau_{\mathrm{ESn}}^{\mathrm{GS}} = \tau_{\mathrm{GSn}}^{\mathrm{ES}} \frac{\mu_{\mathrm{GS}}}{\mu_{\mathrm{ES}}} e^{(E_{\mathrm{ESn}} - E_{\mathrm{GSn}})/k_B T} \quad (5)$$

$$\tau_{\mathrm{WLn}}^{\mathrm{ES}} = \tau_{\mathrm{ESn}}^{\mathrm{WL}} \frac{\mu_{\mathrm{ES}} N_d N_l}{\rho_{\mathrm{WLeff}}} e^{(E_{\mathrm{WL}} - E_{\mathrm{ESn}})/k_B T} \quad (6)$$

$$\tau_{\mathrm{WLn}}^{\mathrm{GS}} = \tau_{\mathrm{GSn}}^{\mathrm{WL}} \frac{\mu_{\mathrm{GS}} N_d N_l}{\rho_{\mathrm{WLeff}}} e^{(E_{\mathrm{WL}} - E_{\mathrm{GSn}})/k_B T} \quad (7)$$

where ρ_{WLeff} is the effective density of states in the WL and E_{WL} is its emission energy. The numerical model is based on the MPRE analysis already reported in [13]. According to all those assumptions the MPRE system, describing the change in carrier number of the three electronic energy levels, can be written as

$$\frac{dN_{\mathrm{WL}}}{dt} = \frac{I}{e} + \sum_n \frac{N_{\mathrm{ESn}}}{\tau_{\mathrm{WLn}}^{\mathrm{ES}}} + \sum_n \frac{N_{\mathrm{GSn}}}{\tau_{\mathrm{WLn}}^{\mathrm{GS}}} - \frac{N_{\mathrm{WL}}}{\tau_{\mathrm{ES}}^{\mathrm{WL}}} - \frac{N_{\mathrm{WL}}}{\tau_{\mathrm{WL}}^{\mathrm{spon}}} - \frac{N_{\mathrm{WL}}}{\tau_{\mathrm{GS}}^{\mathrm{WL}}} \qquad n = 0, 1, \ldots, N-1 \quad (8)$$

$$\frac{dN_{\mathrm{ESn}}}{dt} = \frac{N_{\mathrm{WL}}}{\tau_{\mathrm{ESn}}^{\mathrm{WL}}} + \frac{N_{\mathrm{GSn}}(1 - P_{\mathrm{ESn}})}{\tau_{\mathrm{ESn}}^{\mathrm{GS}}} - \frac{N_{\mathrm{ESn}}}{\tau_{\mathrm{WLn}}^{\mathrm{ES}}} - \frac{N_{\mathrm{ESn}}}{\tau_{\mathrm{GSn}}^{\mathrm{ES}}} - \frac{N_{\mathrm{ES}}}{\tau_{\mathrm{ES}}^{\mathrm{spon}}} - \frac{c\Gamma}{n_r} \sum_m g_{mn\mathrm{ES}} S_m \qquad m = 0, 1, \ldots, M-1 \quad (9)$$

$$\frac{dN_{\mathrm{GSn}}}{dt} = \frac{N_{\mathrm{ESn}}}{\tau_{\mathrm{GSn}}^{\mathrm{ES}}} + \frac{N_{\mathrm{WL}}}{\tau_{\mathrm{GSn}}^{\mathrm{WL}}} - \frac{N_{\mathrm{GSn}}(1 - P_{\mathrm{ESn}})}{\tau_{\mathrm{ESn}}^{\mathrm{GS}}} - \frac{N_{\mathrm{GSn}}}{\tau_{\mathrm{WLn}}^{\mathrm{GS}}} - \frac{N_{\mathrm{GS}}}{\tau_{\mathrm{GS}}^{\mathrm{spon}}} - \frac{c\Gamma}{n_r} \sum_m g_{mn\mathrm{GS}} S_m \qquad m = 0, 1, \ldots, M-1 \quad (10)$$

with N_{WL} being the carrier number in the WL and Γ the optical confinement factor. In order to calculate the entire emission spectrum, the model has been extended considering also the presence of many cavity longitudinal modes, hence the photon number with resonant energy of the mth mode is depicted by S_{m}

$$\frac{dS_m}{dt} = \frac{c\Gamma}{n_r} \sum_n (g_{mn\mathrm{ES}} + g_{mn\mathrm{GS}}) S_m - \frac{S_m}{\tau_p} + \beta \sum_m \left(B_{\mathrm{ES}}(E_m - E_{\mathrm{ESn}}) \frac{N_{\mathrm{ES}}}{\tau_{\mathrm{ES}}^{\mathrm{spon}}} + B_{\mathrm{GS}}(E_m - E_{\mathrm{GSn}}) \frac{N_{\mathrm{GS}}}{\tau_{\mathrm{GS}}^{\mathrm{spon}}} \right) \Delta E_m. \quad (11)$$

The rate of photons emitted out of the cavity is $S_{\mathrm{m}}/\tau_{\mathrm{p}}$, with τ_{p} being the photon lifetime. The contribution of the spontaneous emission to the lasing mode is calculated as the sum of the ES and GS spontaneous transitions multiplied by the spontaneous emission coupling factor β, assumed to be constant. In (9)–(11), the material gain is described by the set of equations

$$g_{mn\mathrm{ES}} = \mu_{\mathrm{ES}} \frac{\pi e^2 \hbar}{c n_r \varepsilon_0 m_0^2} \frac{N_d}{H} \frac{|P_{\mathrm{ES}}^{\sigma}|^2}{E_{\mathrm{ESn}}} \times (2P_{\mathrm{ESn}} - 1) G_{\mathrm{nES}} B_{\mathrm{ES}}(E_m - E_{\mathrm{ESn}}) \quad (12)$$

$$g_{mn\mathrm{GS}} = \mu_{\mathrm{GS}} \frac{\pi e^2 \hbar}{c n_r \varepsilon_0 m_0^2} \frac{N_d}{H} \frac{|P_{\mathrm{GS}}^{\sigma}|^2}{E_{\mathrm{GSn}}} \times (2P_{\mathrm{GSn}} - 1) G_{\mathrm{nGS}} B_{\mathrm{GS}}(E_m - E_{\mathrm{GSn}}). \quad (13)$$

Here, H is the average height of the QD and $|P_{\mathrm{ES,GS}}^{\sigma}|^2$ is the density matrix momentum [21]. Furthermore, let us emphasize that the various QD population are coupled by the homogeneous broadening of the stimulated emission process assumed to be Lorentzian such as

$$B_{\mathrm{ES,GS}}(E_m - E_{\mathrm{ESn,GSn}}) = \frac{\Gamma_{\mathrm{hom}}/2\pi}{(E_m - E_{\mathrm{ESn,GSn}})^2 + (\Gamma_{\mathrm{hom}}/2)^2} \quad (14)$$

with Γ_{hom} being the full-width at half-maximum (FWHM) of the homogeneous broadening and E_{m} being the mode energy. All parameters used in the calculations are summarized in Table I.

In what follows, the MPRE model is applied to model the behavior of InAs–InP(113)B QD laser emitting at 1.55 μm. More particularly, a spectral analysis exhibiting properties linked to the two-state lasing as well as the effects of the cavity length

TABLE I
PARAMETERS OF THE QD MATERIAL AND LASER AT THE RT

QD material parameters	Laser parameters
Emission energy of the WL, E_{WL} = 1.05-eV	Energy separation, E_{ES} - E_{GS} = 47.8meV
Spontaneous emission from WL, $\tau_{WL}^{spon} = 500ps$	Average QD radius, R = 1.55 ·10^{-6} cm
Spontaneous emission from ES, $\tau_{ES}^{spon} = 500ps$	Average QD height, H = 2 ·10^{-7} cm
Spontaneous emission from GS, $\tau_{GS}^{spon} = 1200ps$	QD Surface density, N_d=10^{11} cm^2/QD layer
WL phonon assisted relaxation, $A_W = 1.35 \cdot 10^{10}$ s^{-1}	Number of QD layers, $2 \leq N_l \leq 6$
ES phonon assisted relaxation, $A_E = 1.5 \cdot 10^{10}$ s^{-1}	Optical confinement factor for the QD, $\Gamma = 0.036$
WL Auger coefficient, $C_W = 5 \cdot 10^{-15}$ m^{3}s^{-1}	Mirror reflectivity, $R_1 = R_2 = 0.33$
ES Auger coefficient, $C_E = 9 \cdot 10^{-14}$ m^{3}s^{-1}	Cavity internal losses, α_i = 10-cm^{-1}
GS central energy emission, E_{GS}=0.792eV	Homogeneous broadening 10meV $\leq \Gamma_{hom} \leq$ 30meV
ES central energy transition, E_{ES}=0.840eV	Inhomogeneous broadening, $\Gamma_{inhom} \sim$ 50meV

on the emission of properties are investigated both theoretically and experimentally.

III. NUMERICAL RESULTS AND COMPARISON WITH THE EXPERIMENTS

In this section, numerical results are presented and compared to experiments. The study starts with the calculations of the modal gain for the GS and the ES, respectively, then the investigation of the two-state lasing properties. The last part deals with the influence of the cavity length on the lasing characteristics. In this later case, it is shown that the lasing wavelength shift does not exhibit an abrupt transition unlike InAs–GaAs QD lasers.

A. On the Modal Gain and the Two-State Lasing

Applying the MPRE model, the maximum modal gain due to carriers in the GS (solid line) and in the ES (dashed line) for a 1-mm-long laser with as cleaved facets is calculated and depicted in Fig. 2. The level of total loss, which is represented by the horizontal line, equals $\sim$21 cm^{-1} (assuming internal loss of 10 cm^{-1}, which is a typical value on InP substrates). These simulations show that when the injected current is about $\sim$20 A/cm^2 gain equals loss in the cavity and the GS starts lasing. Then, as far as the injected current increases the GS modal gain saturates at 22.5 cm^{-1}. When the injected current density is increased, the gain of the ES equals loss of the cavity: under this situation both the ES and the GS states coexist in the laser structure. This is the situation where the so-called double laser emission is observed. Finally, when the current density gets higher, the ES emission becomes more important and the GS one saturated. As previously mentioned, recent experimental studies conducted on QD

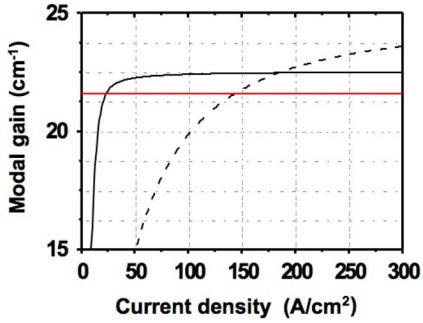

Fig. 2. Modal gain as a function of the current density for the GS (dotted line) and the ES (dashed line), respectively.

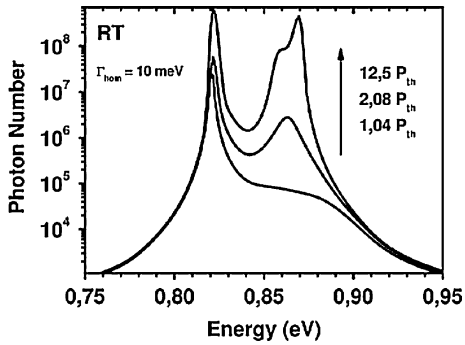

Fig. 3. Calculated optical spectrum at RT.

lasers have shown that a second laser peak appears in the laser spectrum for InAs–GaAs and for InAs–InP systems [9], [10].

More particularly, in the case of the QD lasers grown on InP substrates, it is has been shown in [15] that when a direct relaxation channel from the WL to the GS is taken into account, the impact of the double laser emission on the light current characteristic can be properly explained. For instance, in [15], it has been shown that in GaAs-based lasers, the emission of the GS saturates completely while the ES emission increases linearly. On the other hand, in the case of InP(1 1 3)B-based devices, the relaxation channel from the WL to the GS induces a slight decrease of the GS slope efficiency (but no saturation) while the global slope efficiency increases. As an example, Fig. 3 shows the calculated spectra at room temperature (RT) of a laser diode composed of an active region with six InAs QD stacked layers. The cavity length is 2.45 mm with cleaved uncoated facets while the width of the strip is 120 μm. In the calculations, the homogeneous broadening has been fixed to 10 meV. As it can be seen, the GS laser emission is predicted at 0.82 eV (1.51 μm) for $1.04P_{\rm th}$, $P_{\rm th}$ being the threshold pumping power. With increasing pumping power density the emission intensity increases. Then, a second stimulated emission appears for $2.08P_{\rm th}$ with a laser peak centered at 0.86 eV (1.44 μm). It is worth noting that these numerical results exhibit a very good agreement with experimental ones published in [9].

B. Effect of the Cavity Length on the Lasing Spectrum

In order to analyze the effects of the cavity length on the spectrum characteristics, let us now consider the case of a laser diode composed of an active region with two InAs QD layers. The laser structure consists of a waveguide structure comprising 150 nm lattice-matched GaInAsP with a bandgap

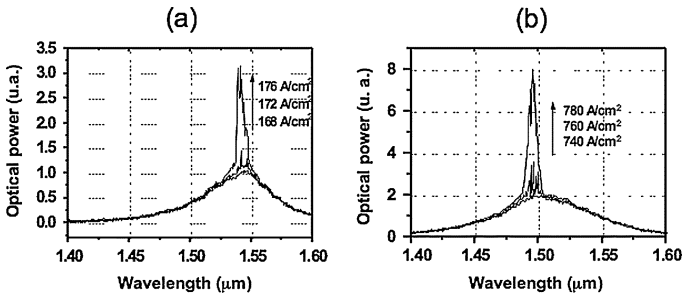

Fig. 4. Measured spectra for two cavity lengths. (a) 3 mm. (b) 1 mm.

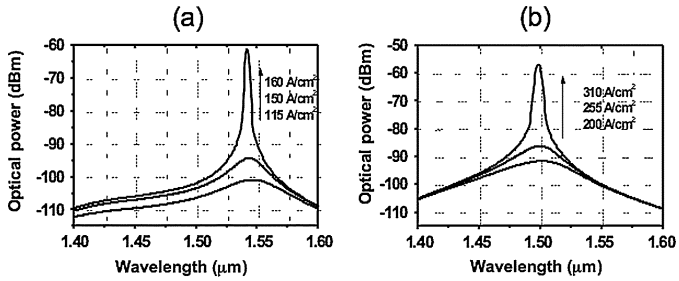

Fig. 5. Calculated spectra for two cavity lengths. (a) 3 mm. (b) 1 mm.

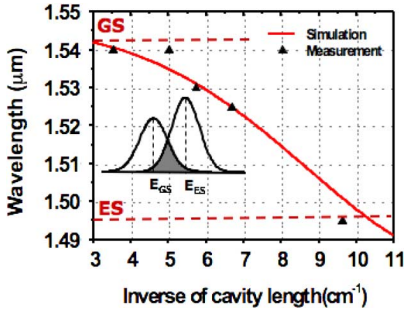

Fig. 6. Lasing wavelength as a function of the inverse of the cavity length.

emission wavelength of 1.18 μm (Q1.18) on both sides of the single layer of InAs QDs, self-assembled through the Stranski–Krastanov growth mode. Conventional edge-emitting laser with a 100-μm-wide ridge structure was formed by wet chemical etching. Long lasers with uncoated as-cleaved facets with an approximate reflectivity of 33% on both sides have been fabricated. In Fig. 4, measured spectra are depicted for two cavity lengths: 3 mm (a) and 1 mm (b). These measurements show that for the longer device, the emitting wavelength is centered at $\sim$1.54 μm, which is the signature of the GS emission. However, when the cavity length goes down to 1 mm the lasing takes place only from ES transition at $\sim$1.49μm. It is, however, important to stress that despite the main contribution in the lasing wavelength comes from the ES, the smaller dots also contribute with their GS at the lasing wavelength.

Compare to Fig. 2 in which a GS lasing emission is predicted for the same cavity length and for a pump current as low as 20 A/cm^2, Fig. 4(b) shows a direct emission on the ES. This difference can be attributed to a higher loss level. It has been recently shown that the internal loss on InP can range from 10 to 19 cm^{-1} [22]. Consequently, when considering internal loss of 12 cm^{-1} (instead of 10 cm^{-1}) no GS emission can occur in Fig. 2 and the laser emits directly on the ES, as shown in Fig. 4(b).

Also in Fig. 4, it is shown that a higher threshold current density is required ($\sim$700 A/cm^2) for the shorter device emitting on the ES that the one emitting on the GS ($\sim$300 A/cm^2). This effect can be attributed to the higher number of eh-pairs needed to obtain transparency in the ES than on the GS due to the degeneracy difference.

In Fig. 5, calculated spectra corresponding to the measured results of Fig. 4 are depicted. The internal loss value has been adjusted to match the experimental observations in Fig. 4(b). As it can be seen, a very good agreement between simulations and measurements is obtained. The simulation well reproduces the influence of the cavity length on the lasing wavelength. It is important to stress that the calculated current densities are in a slight disagreement with those depicted in Fig. 4. For instance, the current density is about 750 A/cm^2 in Fig. 4(b) instead of $\sim$300 A/cm^2 for the calculations in Fig. 5(b). We believe such a difference may come from leakage currents, which are not included in the model meaning that values of current densities are probably underestimated in the calculations.

In order to analyze how the transition behaves from the GS to ES, Fig. 6 shows the variation of the lasing wavelength as a function of the inverse of the cavity length. This effect can be also studied by considering devices of the same length, but with different facet coatings to modify losses at transparency: GS lasing should occur with high-reflection coating, and successive GS and ES lasing should appear for intermediate reflection coefficients. This last option has not been investigated in what follows. All laser diodes are composed of an active region with two InAs QD layers. The cavity length ranges from $\sim$3 mm down to $\sim$1 mm. Black triangular points are obtained from measurements while the red solid line is obtained from the calculations of the optical spectra.

As it can be seen for longer cavity lengths, i.e., $1/L \sim$ 3–4 cm^{-1} ($L \sim$ 2.5–3 mm), the lasing wavelength remains almost constant located at the GS transition around 1.54 μm [see Fig. 6(a)]. Then, when decreasing the cavity length below 2 mm (i.e., $1/L \sim 5$ cm^{-1}), the lasing wavelength slightly shifts down to 1.49 μm [see Fig. 5(b)] that corresponds to the 1-mm-long cavity ($1/L \sim 10$ cm^{-1}). Consequently, this result demonstrates that in the case of InAs–InP(113)B QD lasers, a continuous transition from the GS toward the ES is predicted. The GS always contributes to lasing emission but its contribution decreases as long as the lasing wavelength moves from longer to shorter wavelength.

This result is strengthened by the fact that both calculations and experimental results are in a relative good agreement. It is important to emphasize that this effect has also been observed on a similar structure with three QD layers [8]. However, to our knowledge such a comparison with calculations has not been reported yet.

This continuous transition has never been observed in the InAs–GaAs system since lasing wavelength switches drastically on the ES as reported in [11] and [23]. This is because the spreading in QD size distribution in InAs–GaAs system is not as important as in the InAs–InP system. The inhomogeneous broadening is about 40–50 meV instead of $\sim$70 meV at RT on InP substrates. Furthermore, a better carrier confinement into the dots is usually obtained on GaAs and this determines a larger energy separation between the GS and the ES ($\sim$70 meV) compare to the InAs–InP system ($\sim$30 meV). Consequently, in the

InAs–InP system, a spectral overlap between the GS and the ES gain occurs as sketched in the inset of Fig. 6. As a consequence of the significant gain overlap, a continuous variation of the gain peak from the GS to the ES energy when current density is increased. As a conclusion, the use of a numerical model based on MPRE has served to demonstrate that the characteristics of 1.55 μm InAs–InP(113)B QD lasers are different compare to 1.31 μm InAs–GaAs QD device ones. Especially, a continuous transition for the lasing wavelength from the GS to the ES is reported when reducing the cavity length.

IV. Conclusion

In this paper, a theoretical model has been used to investigate the lasing spectrum properties of InAs–InP(113)B QD lasers emitting at 1.55 μm. The numerical model is based on an MPRE analysis and takes into account the QD size dispersion as well as the temperature dependence through both the inhomogeneous and the homogeneous broadenings. Especially, this paper has highlighted the influence of the cavity length on the lasing wavelength. As a consequence, optical spectra have been calculated for different cavity loss levels. Because of the spectral overlap between the GS and the ES gain occurring in InAs–InP(113)B QD devices, simulations have demonstrated in agreement with the experiments that the gain peak shifts continuously from the GS to the ES energy when current density is increased. As a conclusion, this numerical tool opens the way of predicting the behavior of InAs–InP(113)B QD lasers emitting at 1.55 μm that have recently shown improved performances [24]. This numerical investigation based on carrier dynamics is of prime importance for the optimization of low-cost sources for optical telecommunications as well as for a further improvement of QD laser performances at 1.55 μm on InP substrate.

References

[1] G. T. Liu, A. Stintz, H. Li, K. J. Malloy, and L. F. Lester, "Extremely low room-temperature threshold current density diode lasers using InAs dots in $In_{0.15}Ga_{0.85}As$ quantum well," *Electron. Lett.*, vol. 35, no. 14, pp. 1163–1165, 1999.

[2] S. S. Mikhrin, A. R. Kovsh, I. L. Krestnikov, A. V. Kozhukhov, D. A. Livshits, N. N. Ledentsov, Yu. M. Shernyakov, I. I. Novikov, M. V. Maximov, V. M. Ustinov, and Zh. I. Alferov, "High power temperature-insensitive 1.3 μm InAs/InGaAs/GaAs quantum dot lasers," *Semicond. Sci. Technol.*, vol. 20, pp. 340–342, 2005.

[3] H. Saito, K. Nishi, A. Kamei, and S. Sugou, "Low chirp observed in directly modulated quantum dot lasers," *IEEE Photon. Technol. Lett.*, vol. 12, no. 10, pp. 1298–1300, Oct. 2000.

[4] D. O'Brien, S. P. Hegarty, G. Huyet, J. G. McInerney, T. Kettler, M. Laemmlin, D. Bimberg, V. M. Ustinov, A. E. Zhukov, S. S. Mikhrin, and A. R. Kovsh, "Feedback sensitivity of 1.3 μm InAs/GaAs quantum dot lasers," *Electron. Lett.*, vol. 39, no. 25, pp. 1819–1820, 2003.

[5] M. Grundmann, O. Stier, S. Bognar, C. Ribbat, F. Heinrichsdorff, and D. Bimberg, "Optical properties of self-organized quantum dots: Modelling and experiments," *Phys. Status Solidi A*, vol. 178, pp. 255–262, 2000.

[6] H. Hatori, M. Sugawara, K. Mukai, Y. Nakata, and H. Ishikawa, "Room-temperature gain and differential gain characteristics of self-assembled InGaAs/GaAs quantum dots for 1.1–1.3 μm semiconductor laser," *Appl. Phys. Lett.*, vol. 77, no. 6, pp. 773–775, 2000.

[7] L. Ya. Karachinsky, T. Kettler, N. Yu. Gordeev, I. I. Novikov, M. V. Maximov, Yu. M. Shernyakov, N. V. Kryzhanovskaya, A. E. Zhukov, E. S. Semenova, A. P. Vasil'ev, V. M. Ustinov, N. N. Ledentsov, A. R. Kovsh, V. A. Shchukin, S. S. Mikhrin, A. Lochmann, O. Schulz, L. Reissmann, and D. Bimberg, "High-power singlemode CW operation of 1.5 μm range quantum dot GaAs-based laser," *Electron. Lett.*, vol. 41, no. 8, pp. 478–480, 2005.

[8] P. Caroff, C. Paranthoën, C. Platz, O. Dehaese, H. Folliot, N. Bertru, C. Labbé, R. Piron, E. Homeyer, A. Le Corre, and S. Loualiche, "High gain and low threshold InAs quantum dot lasers on InP," *Appl. Phys. Lett.*, vol. 87, pp. 243107-1–243107-3, 2005.

[9] C. Platz, C. Paranthoen, P. Caroff, N. Bertru, C. Labbe, J. Even, O. Dehaese, H. Folliot, A. Le Corre, S. Loualiche, G. Moreau, J. C. Simon, and A. Ramdane, "Comparison of InAs quantum dot lasers emitting at 1.55 μm under optical and electrical injection," *Semicond. Sci. Technol.*, vol. 20, pp. 459–463, 2005.

[10] M. Sugawara, N. Hatori, H. Ebe, Y. Arakawa, T. Akiyama, K. Otsubo, and Y. Nakata, "Modelling room-temperature lasing spectra of 1.3 μm selfassembled InAs/GaAs quantum-dot lasers: Homogeneous broadening of optical gain under current injection," *J. Appl. Phys.*, vol. 97, pp. 043523-1–043523-8, 2005.

[11] A. Markus, J. X. Chen, C. Paranthoen, A. Fiore, C. Platz, and O. Gauthier-Lafaye, "Simultaneous two-state lasing in quantum-dot lasers," *Appl. Phys. Lett.*, vol. 82, no. 12, pp. 1818–1820, 2003.

[12] A. Markus, J. X. Chen, O. Gauthier-Lafaye, J. Provost, C. Paranthoën, and A. Fiore, "Impact of intraband relaxation on the performance of a quantum-dot laser," *IEEE J. Sel. Topics Quantum Electron.*, vol. 9, no. 5, pp. 1308–1314, Sep./Oct. 2003.

[13] M. Gioannini, A. Sevega, and I. Montrosset, "Simulations of differential gain and linewidth enhancement factor of quantum dot semiconductor lasers," *Opt. Quantum Electron.*, vol. 38, pp. 381–394, 2006.

[14] E. A. Viktorov, P. Mandel, Y. Tanguy, J. Houlihan, and G. Huyet, "Electron–hole asymmetry and two-state lasing in quantum dot lasers," *Appl. Phys. Lett.*, vol. 87, pp. 053113-1–053113-3, 2005.

[15] K. Veselinov, F. Grillot, C. Cornet, J. Even, A. Bekiarski, M. Gioannini, and S. Loualiche, "Analysis of the double laser emission occurring in 1.55 μm InAs-InP(1 1 3)B quantum-dot lasers," *IEEE J. Quantum Electron.*, vol. 43, no. 9, pp. 810–816, Sep. 2007.

[16] B. Dagens, O. Bertran-Pardo, M. Fischer, F. Gerschutz, J. Koeth, I. Krestnikov, A. Kovsh, O. Le Gouezigou, and D. Make, "Uncooled directly modulated quantum dot laser 10 Gb/s transmission at 1.3 μm, with constant operation parameters," presented at the Eur. Conf. Opt. Commun., Cannes, France, 2006, Th. 4.5.7.

[17] F. Gershutz, M. Fischer, J. Koeth, M. Chacinski, R. Schatz, O. Kjebon, A. Kovsh, I. Krestinkov, and A. Forschel, "Temperature insensitive 1.3/spl mu/InGaAs=GaAs quantum dot distributed feedback lasers for 10 Gbit=s transmission over 21 km," *Electron. Lett.*, vol. 42, no. 25, pp. 1457–1458, 2006.

[18] P. Miska, C. Paranthoen, J. Even, O. Dehaese, H. Folliot, N. Bertru, S. Loualiche, M. Senes, and X. Marie, "Optical spectroscopy and modelling of double-cap grown InAs/InP quantum dots with long wavelength emission," *Semicond. Sci. Technol.*, vol. 17, pp. L63–L67, 2002.

[19] B. Ohnesorge, M. Albrecht, J. Oshinowo, Y. Arakawa, and A. Forchel, "Rapid carrier relaxation in self-assembled $In_xGa_{1-x}As$/GaAs quantum dots," *Phys. Rev. B*, vol. 54, no. 16, pp. 11532–11538, 1996.

[20] T. Berg, S. Bischoff, I. Magnusdottir, and J. Mork, "Ultrafast gain recovery and modulation limitations in self-assembled quantum-dot devices," *IEEE Photon. Technol. Lett.*, vol. 13, no. 6, pp. 541–543, Jun. 2001.

[21] M. Sugawara, K. Mukai, Y. Nakata, and H. Ishikawa, "Effect of homogeneous broadening of optical gain on lasing spectra in self-assembled $In_xGa_{1-x}As$/GaAs quantum dot lasers," *Phys. Rev. B.*, vol. 61, no. 11, pp. 7595–7603, 2000.

[22] D. Zhou, R. Piron, F. Grillot, O. Dehaese, E. Homeyer, M. Dontabactouny, T. Batte, K. Tavernier, J. Even, and S. Loualiche, "Study of the characteristics of 1.55 μm quantum dash/dot semiconductor lasers on InP substrate," *Appl. Phys. Lett.*, vol. 93, pp. 161104-1–161104-3, 2008.

[23] A. E. Zhukov, A. R. Kovsh, V. M. Ustinov, Yu. M. Shernyakov, S. S. Mikhrin, N. A. Maleev, E. Yu. Kondrat'eva, D. A. Livshits, M. V. Maximov, B. V. Volovik, D. A. Bedarev, Yu. G. Musikhin, N. N. Ledentsov, P. S. Kop'ev, Z. I. Alferov, and D. Bimberg, "Continuous-wave operation of long-wavelength quantum-dot diode laser on a GaAs substrate," *IEEE Photon. Technol. Lett.*, vol. 11, no. 11, pp. 1345–1347, Nov. 1999.

[24] A. Martinez, K. Merghem, S. Bouchoule, G. Moreau, A. Ramdane, J.-G. Provost, F. Alexandre, F. Grillot, O. Dehaese, R. Piron, and S. Loualiche, "Dynamic properties of InAs/InP(311B) quantum dot Fabry–Perot lasers emitting at 1.52-μm," *Appl. Phys. Lett.*, vol. 93, pp. 021101-1–021101-3, 2008.

Frédéric Grillot (S'02–M'02) was born in Versailles, France, on August 22, 1974. He received the M.Sc. degree in physics from Dijon University, Dijon, France, in 1999 and the Ph.D. degree in electrical engineering from Besançon University, Besançon, France, in 2003. His doctoral research activities were conducted within the optical component research department in Alcatel. Along with his Ph.D., he studied the effects of the optical feedback in semiconductor lasers, and the impact this phenomenon has on optical communication systems for high bite rate transmissions.

From May 2003 to August 2004, he was working with the Institut d'Electronique Fondamentale, University of Paris-Sud, where he focused on integrated optics modeling and on Si-based passive devices for optical interconnects and telecommunications. On September 1, 2004, he had been appointed to the Institut National des Sciences Appliquées de Rennes (INSA) where he is currently working as an Associate Professor within the Materials and Nanotechnologies (MNT) Department. His main research activities are on advanced laser diodes emitting at 1.55-μm using new materials like quantum dots for low-cost applications. Since 2008, he has also been a Visiting Research Professor of Electrical and Computer Engineering at the University of New Mexico. He is leading Research in optical science and optoelectronics at the Center for High Technology Materials (CHTM).

Dr. Grillot is a member of the IEEE Photonics Society (formerly the Lasers and Electro-Optics Society), SPIE, and la Société Française d'Optique.

Kiril Veselinov (S'07–M'07) was born in Sofia, Bulgaria, in 1978. He received the M.S. degree in electrical engineering from Technical University of Sofia, Bulgaria, in 2002. He is currently working toward the Ph.D. degree at Fonctions Optiques pour les Technologies de l'informatiON-Institut National des Sciences Appliquées (FOTON-INSA), Rennes, France.

He is currently with the Department of Materials and Nanotechnology, National Institute of Applied Sciences, Rennes, France. His current research interests include modeling and characterization of semiconductor lasers and optical amplifiers. Since 2004, his current research interests include modeling of quantum dot materials and lasers.

Mariangela Gioannini (M'07) was born in Cuorgnè, Italy, in 1973. She received the M.S. degree in electronic engineering and the Ph.D. degree in electronic and communication engineering from Politecnico di Torino, Torino, Italy, in 1998 and 2002, respectively.

Since 2002, she has been with the Dipartimento di Elettronica, Politecnico di Torino, first in a Post-Doctoral position and then as a permanent Researcher since January 2005. She was a Visiting Researcher with the University of Bristol, Bristol, U.K., in 2001, and at the Fraunhofer Institut fur Nachrichtentechnik, Heinrich-Hertz-Institut, Berlin, Germany, in 2001 and 2002. Her current research interests include modeling and characterization of semiconductor lasers and optical amplifiers. Since 2002, she has been engaged in modeling of quantum-dot and quantum-dash materials, lasers, and optical amplifiers.

Ivo Montrosset (M'92) was born in Aosta, Italy, in 1946. He received the Laurea degree in electronic engineering from the Politecnico di Torino, Torino, Italy, in 1971.

From 1972 to 1986, he was with the Politecnico di Torino. In 1986, he was appointed as a Full Professor at the Universita' di Genova, Genova, Italy. Since 1990, he has been a Full Professor of optoelectronics with Politecnico di Torino. His current research interests include the field of guided-wave optics, solid-state and semiconductor lasers, and other related topics.

Jacky Even was born in Rennes, France, in 1964. He received the Ph.D. degree from the University of Rennes I, Rennes, in 1992.

From 1992 to 1999, he was a Research and Teaching Assistant with the University of Rennes I. Since 1999, he has been a Full Professor of optoelectronics with the Institut National des Sciences Appliquées (INSA), Rennes. His current research interests include the theoretical study of the electronic, optical, and nonlinear properties of quantum-well and quantum-dot structures and the simulation of optoelectronic devices. He is the author or coauthor of 80 papers.

Rozenn Piron was born in Paris, France, in 1975. She received the Ph.D. degree from the Ecole Normale Supérieure de Cachan (ENS-Cachan), Cachan, France, in 2002. Her doctoral research focused on all-optical poling and nonlinear optical effects in polymer-based microcavities dedicated to optical telecommunication applications.

Her doctoral work was performed at the Laboratory LPQM (UMR CNRS 8527) and supported by France Telecom R&D. From 2002 to 2004, she held a postdoctoral position with SATIE-BIOMIS (UMR CNRS 8029) at ENS-Cachan, antenne de Bretagne, Bruz, France. Her research activities were on cell biochips development for biological applications and cover clean-room processing and characterization of biomicrosystems. In September 2004, she joined the FOTON Laboratory (UMR CNRS 6082) at the Institut National des Sciences Appliquees (INSA), Rennes, France, where she is now a Lecturer within the Materials and Nanotechnologies (MNT) Department. Her research activities are focused on optoelectronic devices based on III/V semiconductor nanostructures [quantum dots (QD) and quantum dashes (QDH)] for telecommunication applications. She is mainly involved in characterization of 1.55-μm QD and QDH devices (e.g., lasers and mode-locked lasers).

Estelle Homeyer graduated from the Ecole Nationale Supérieure de Physique and received the M.S. degree in physics from the Louis Pasteur University of Strasbourg in 2004 and the Ph.D. degree from FOTON (Optical Function for Telecommunication) Laboratory, Rennes, France, in 2007. Her doctoral work focused on electrooptical properties of InAs–InP quantum dot lasers.

After a year of postdoctoral work on infrared properties of InAs–GaAs quantum dots polarons at the Institute of Fundamental Electronics, Paris, she has now joined the Nanostructures for Optics team with the Laboratory of Condensed Matter Physics and Nanostructures, Université Claude Bernard Lyon 1 and CNRS, Villeurbanne, France.

Slimane Loualiche was born in Ouacif, Algeria, in 1950. He graduated from Ecole Supérieur d'Electricité de Paris, Paris, France, in 1975. He received the Ph.D. degree from Ecole Normale Superieure de Paris in 1979.

He is a Full Professor of Optoelectronics at the Institut National des Sciences Appliquées (INSA), Rennes, France, and the Head of the Fonctions Optiques pour les Technologies de l'informatiON (FOTON)-INSA, Rennes. His current research interests include the experimental and theoretical study of the optical and dynamical properties of quantum-well (QW) and quantum-dot (QD) structures, using, in particular, Fourier transform absorption and pump and probe techniques. He also has a long experience with the epitaxial growth, characterization, and modeling of the properties of nanostructures (QW and QD) and devices. He is the author or coauthor of more than 160 scientific papers and 11 patents.